Toxicology Reports 12 (2024) 10–17

Contents lists available at ScienceDirect

Toxicology Reports

journal homepage: www.elsevier.com/locate/toxrep

# Silver nanoparticles induces apoptosis of cancer stem cells in head and neck cancer

Rupinder Kaur, Khushwant Singh, Sonam Agarwal, Marilyn Masih, Anita Chauhan, Pramod Kumar Gautam *

*Department of Biochemistry, All India Institute of Medical Sciences, New Delhi 110029, India*

ARTICLE INFO

Handling Editor: Prof. L.H. Lash

*Keywords:*
AgNPs
CSCs
Cell Cycle
Apoptosis
Anti-cancer
Cell viability

ABSTRACT

*Background:* Several nano formulations of silver nanoparticles with bioconjugates, herbal extracts and anti-cancerous drug coating have been vividly studied to target cancer. Despite of such extensive studies, AgNPs (silver nanoparticles) have not reached the stage of clinical use. Out of all possible reasons for this failure, the unexplored effect on Cancer Stem Cell (CSC) population and mechanism of action of AgNPs, are the most plausible ones and are worked upon in this study.

*Methods:* AgNPs were synthesized by chemical reduction method using sodium citrate and characterized by UV, FTIR, XRD and electron microscopy. CSC population was isolated from Cal33 cell line by MACS technique. MTT assay, trypan blue exclusion assay, Annexin V and PI based apoptosis assay and cell cycle assay were performed.

*Results:* The results showed that synthesized AgNPs have cytotoxic activity on all cancer cell lines tested with the $IC_{50}$ value of a wide range (1.5–49.21 μg/ml for cell lines and 0.0643–0.1211 μg/ml for splenocytes and thymocytes). CSCs Cal33 showed higher resistance to AgNP treatment and arrest in G1/G0 phase upon cell cycle analysis.

*Conclusion:* AgNPs as an anti-cancer agent although have great potential but is limited by its off-target effects on normal cells and less effective on cancer stem cells at lower concentrations.

## 1. Introduction

Global cancer burden is a second leading death cause among other causes of death worldwide and raising serious concerns to devise immediate prevention or cure methods to reduce the burden of this devastating disease [1]. Over the last two decades silver nanoparticles (AgNPs) have been widely used in cancer therapeutic studies. They have been known for a long time to have potent anti-microbial, antiviral and anti-cancerous activity [2,3]. Numerous studies have been performed on anti-tumor potential of chemically synthesized of AgNPs [4,5], herbal plant extract synthesized AgNPs[6], bio-conjugated AgNPs [7] and drug coated AgNPs as nanocarriers on cancer cells [8]. However, the mechanisms underlying this activity are not yet completely understood[9] and need further investigation. Surprisingly, such studies have ignored the effect of sliver monotherapies on CSC population and immune cell population surrounding the tumor site. CSCs present at tumor site have similar characteristics as normal stem or progenitor cells such as self-renewal ability and multi-lineage differentiation to drive tumor growth [10]. Challengingly, conventional cancer treatments target the bulk of the tumor and are unable to specifically target CSCs due to their highly resistance nature, leading to metastasis and tumor recurrence [11]. A study on differential cytotoxic potential of *E. coli* derived silver nanoparticles in human ovarian cancer cells and ovarian cancer stem cells reported increased sensitivity of cancer stem cells than bulk cells [12]. Another study has established that *E. coli* derived AgNP treatment on F9 teratocarcinoma stem cells induced neuronal differentiation by upregulating biomarkers, such as RBP, laminin B1, and collagen type IV, and downregulating various pluripotency markers, including Nanog, Sox2, and Oct3/4, which are critical transcription factors involved in self-renewal and differentiation. It was also reported that AgNPs could regulate both apoptosis and differentiation by modulating various signaling molecules in a concentration-dependent manner[13]. Only a few studies have highlighted the role of silver nanoparticles on CSCs. This knowledge gap in evaluating the effect of AgNPs therapeutics in

* Corresponding author.
*E-mail addresses:* rupinder.blassi@gmail.com (R. Kaur), skhushwant910@gmail.com (K. Singh), sonam.2mits@gmail.com (S. Agarwal), drmarilynmasih13@gmail.com (M. Masih), rajpootanita09@gmail.com (A. Chauhan), gautam@aiims.edu (P.K. Gautam).

https://doi.org/10.1016/j.toxrep.2023.11.008
Received 20 September 2023; Received in revised form 20 November 2023; Accepted 23 November 2023
Available online 28 November 2023

targeting CSCs subpopulations of tumor microenvironment is a major drawback of nanomaterial related cancer therapies. However, carrying out studies investigating the biology of this heterogenous population of cancer stem cells present in tumor bulk, will open up new frames for targeted nano therapies and decrease the chance of disease recurrence. Therefore, with the aim of elucidating the effect of AgNPs on cancer stem cells as well as their effects on immune cells present in spleen and thymus, In the present study, we explored the antitumor effect of AgNPs on Cal33-a head & neck cancer cell line, Dalton's lymphoma cell line (DL), Breast cancer cell line (MDAMB 231 and MCF7) and PC-3 -a prostate cancer cell line. Since the treatment on Cal33 was most effective at lowest concentrations CSCs harvested from this cell line were tested under the effect of AgNPs to study the sensitivity of cancer stems under nanoparticle treatment. As a control, HEK-293 T cell line was used, splenocytes and thymocytes from Swiss albino mice were also tested under AgNP treatment. Apoptosis assay and cell cycle analysis was also performed on Cal33 and CSCs harvested from Cal33 to elucidate the mode of action of AgNPs in cancer stem cells.

## 2. Materials and methods

### 2.1. Reagents

Silver nitrate was purchased from SRL, India, Sodium citrate and MTT were purchased from Sigma Aldrich, Bangalore, India. DMEM and RPMI 1640 culture medium was obtained from Hi Media, Mumbai, India. Fetal bovine serum (FBS) was obtained from Invitrogen, CA, USA. FITC Annexin V Apoptosis Detection Kit (Cat no. 640914) was purchased from BD Bioscience, MagCellect Streptavidin Ferrofluid (Cat no. MAG999B), CD24 Biotinylated Antibody (Cat no. FAB52471B), Human CD24 APC-conjugated Antibody (Cat no. FAB5247A) and Human CD44 PE-conjugated Antibody (Cat no. FAB8547P) from R&D Systems Minneapolis, Minnesota, United States. CD44 Biotinylated Antibody (Cat no. MA5–17876) was obtained from Thermo Fisher Scientific, Waltham, Massachusetts, United States.

### 2.2. Animal and tumor model

All experiments were done on 2-D monolayer cell lines purchased from the cell repository of NCSS, Pune. Mice experiments were carried on inbred populations of Swiss albino strain of mice of either sex and at 8–12 weeks of age. Mice were obtained from the Animal House, AIIMS, New Delhi, and housed in a pathogen-free specialized small animal facility with a 12 h dark–light cycle. All the animals were treated with utmost human care and had free access to food and water. Mice were euthanized by cervical dislocation, a method authorized by Institutional Animal Ethical Committee (File no- 100/IAEC-1/2018), AIIMS, New Delhi for sacrificing experimental animals, and observed until all muscle activity and breathing has ceased for at least 120 s [14].

### 2.3. Isolation of splenocytes and thymocytes from mice and Cell line culture

Cal33, Dalton's lymphoma (DL), MDAMB 231, MCF7, PC-3 and HEK-293 T cell lines were cultured in their respective medium supplemented with 10% FBS and 1% penicillin-streptomycin (Supplementary figure 2). Mice after euthanization was dissected in sterile conditions to separate spleen and thymus (remaining body parts were utilized for other experiments). Both spleen and thymus were washed with sterile PBS. Each organ was crushed between the coarse side of two glass slides. Resulting mass was dissolved in PBS and cells thus released were filtered by using a cell strainer. Cells were washed with PBS twice and later treated with RBC lysis buffer for 10 mins at room temperature. PBS washing was again given to eliminate RBCs completely. The cell pellet obtained was dissolved in RPMI supplemented with 10% FBS media and kept in 5% $CO_2$ incubator at 37 ℃.

### 2.4. Synthesis and characterization of AgNPs

AgNPs were synthesized by chemical reduction method. 2 ml silver nitrate (0.001 M) was added drop wise to the 30 ml solution of stirred and cool sodium citrate (0.002 M) of double distilled water. Reduction of the silver ion into AgNPs during exposure to the trisodium citrate was indicated by color change, from transparent to golden yellow color in aqueous medium due to the surface plasmon resonance phenomenon [15,16] (Supplementary figure 1). Further, UV spectra (Tecan multimode reader on SparkControl application) were taken at a different time interval. After synthesis of AgNPs, the whole supernatant was collected and centrifuged at 11500 rpm for 15 min at 4 °C, the supernatant was discarded and pellet was washed with distilled water thrice and the final pellet suspended in distilled water such that no unreacted silver ions remain. The nanoparticles were then sonicated and lyophilized. After that powder was collected for performing analytical techniques. FT-IR (Perkin Elmer, Spectrum Two FTIR, Waltham, MA, USA) to identify the possible reducing and stabilizing molecules in Sodium citrate solution, with spectral range from 400 to 4000 $cm^{-1}$ and resolution of 4 $cm^{-1}$, XRD (X'Pert Pro PANalytical, ALMELO, Netherlands) to identify the specimen's crystalline phases and to measure its structural properties, size and orientation of crystalline profile, at 45 kV and 40 mA with 2θ in the range from 0° to 80° angle, NTA (NanoSight NTA 3.1, Malvern Panalytical, UK) to study the particle size distribution in the nanoparticle solution based on its Brownian motion under the light and TEM (Tecnai 20G2 FEI, Oregon, USA) to visualize the size and shape of the nanoparticles.

### 2.5. Isolation and purification of cancer stem cells

Cancer stem cells were isolated from Cal33 cell line by MACs (Magnetic Assisted Cell Sorting technique). Isolation of human $CD24low^{/-}CD44^{+}$ cancer stem cells was done using a two-step procedure. CD24low/- cells were initially isolated by negative selection and then $CD44^{+}$ cells were isolated by positive selection from the $CD24low^{/-}$ cell fraction. Single cell suspension of cells was prepared by traditional methods at a cell density of $1 \times 10^{7}$ cells/ml. 2. $5 \times 10^{6}$ cells were taken in a conical tube and 25 μL of Human CD24 Biotinylated Antibody was added and gently mixed, avoiding bubble formation, and incubated at 2–8 °C in a refrigerator for 15 min. The cell suspension was washed by adding 1 ml of wash buffer and centrifuged at 300 x g for 8 min. The supernatant was removed and cells were resuspended in cold was buffer. 50 μL of Streptavidin Ferrofluid was added to the cell suspension, mix gently and incubated at 2–8 °C in a refrigerator for 15 min. Later, the cell suspension was washed by adding 1 ml of wash buffer and centrifuged at 300 x g for 8 min. The supernatant was removed and cells were resuspended in cold wash buffer. The reaction tube was placed in the magnetic stand and incubated for 8 min at RT. Magnetically tagged $CD24^{+}$ cells migrated toward the magnet (unwanted cells), leaving untagged CD24low/- cells in suspension. While the tube was in the magnet stand, all of the reaction suspension (desired) was carefully aspirated and transferred in a new tube. The tube containing the magnetically selected cells from the magnet was removed and discarded. CD24low/- cells thus obtained was treated with above procedure by replacing the CD24 antibody with Human CD44 Biotinylated Antibody. Magnetically tagged $CD44^{+}$ cells migrated toward the magnet leaving the untagged CD44- cells in suspension in the supernatant. While the tube is in the magnet, all of the reaction suspension (unwanted) was carefully aspirated and discarded. The tube containing the magnetically selected cells was removed from the magnet and resuspend cells by adding 100–500 μL of cold Buffer. This final magnetically isolated fraction contained the desired isolated $CD24^{low/-}$ $CD44^{+}$ cells. The cells were used in downstream applications.

### 2.6. Characterization of CSCs by flowcytometry

After successfully sorting the desired cell population, cells were stained by taking 100 μL of the positively selected cells to a tube 10 μL of the APC-conjugated Human CD24 Detection Antibody and 10 μL of the PE-conjugated Human CD44 Detection Antibody was added and incubated for 30 min at 2–8 °C. Following this incubation, unreacted antibody was removed by washing the cells twice in 2 ml of PBS. Cells were resuspended in 200–400 μL of PBS for final flow cytometric analysis. Compensation controls were also prepared along with the samples.

### 2.7. AgNP treatment and cell viability assay

The AgNPs stock was made in sterile water. Cells were treated with different concentrations of AgNPs. Cell viability of adherent cell lines was determined by MTT assay. $5 \times 10^3$ cells were seeded in each well of 96-well culture plate after 24 hr, cells were treated with 200–1.3 μg/ml concentrations (serial dilutions) of AgNPs in serum free media for 24 hr. and culture medium alone as control. After completion of the incubation period, 10 μL/well (5 mg/ml) of MTT solution was added for 4 hr hours. After 4 hr of incubation period supernatant was discarded and formed formazan crystal was dissolved by adding DMSO and absorbance measured at 570 nm [14,17].

Cell viability of splenocytes and thymocytes was determined by trypan blue exclusion assay. Cells were treated with AgNPs concentration (300–30 ng/ml). After 24-hour treatment the cells were washed and resuspend in 1 ml PBS or serum-free complete medium.1 part of 0.4% trypan blue and 1 part cell suspension was mixed and kept for 3–4 mins at room temperature. 10ul of the trypan blue/cell mixture was loaded on to a hemocytometer. Using a bright field inverted microscope unstained (viable) and stained (nonviable) cells were counted separately. To obtain the total number of viable cells per ml of aliquot, the total number of viable cells was multiplied by 2 (the dilution factor for trypan blue) and for total number of cells per ml of aliquot, viable cells and nonviable cells were added and multiplied by 2 (the dilution factor for trypan blue) [18]. Percentage of viable cells was calculated as follows.

$$\text{Viable cells}(\%) = \frac{\text{total number of viable cells per ml of aliquot}}{\text{total number of cells per ml of aliquot}} X100$$

### 2.8. Apoptosis assay

Cells were treated with AgNPs at their respective $IC_{50}$ concentrations. The treated cells and untreated control cells were washed twice with cell staining buffer, and then resuspend cells in Annexin V binding buffer at a concentration of $0.25–1.0 \times 10^7$ cells/ml .100 μL of cell suspension was transferred in a tube and 5 μL of FITC Annexin V and 10 μL of Propidium Iodide Solution was added. The cells were gently vortexed and incubated for 15 min at room temperature (25 °C) in the dark. 400 μL of Annexin V Binding Buffer was added to each tube and analyzed by flow cytometry [14].

### 2.9. Cell cycle assay

Cells were harvested in PBS and fixed in cold 70% ethanol (adding drop wise to the pellet while vertexing). Fixed cells were kept for 30 min at 4 °C. After incubation cells were washed twice in PBS. The fixed cells were treated with ribonuclease 50 μL of a 100 μg/ml stock of RNase. This ensured only DNA, not RNA, is stained. 200 μL PI (from 50 μg/ml stock solution) was added in kept for one hour at 4 °C in dark. Cells were analyzed using flow cytometry.

### 2.10. Statistical analysis

Each value represents the mean of three independent experiments in each group were conducted. Data was analyzed by using two-tailed student's t-test on statistical software package Graphpad prism 9. A value of $p < 0.05$ was considered significant. Flow cytometry experiments were analyzed using FlowJo software.

## 3. Results and discussion

In the present study, we first time reported the antitumor effect of AgNPs on CSCs harvested from CAL-33 a head & neck cancer cell line and normal Cal33 cells along with Dalton's lymphoma cell line (DL), Breast cancer cell line (MDAMB 231 and MCF7) and a PC-3 prostate cancer cell line. As a control, we used HEK-293 T, Splenocytes and Thymocytes. Apoptosis and cell cycle was performed on CSCs harvested form Cal33.

Sodium Citrate induced synthesis of AgNPs was primarily confirmed by the appearance of golden yellow color. The changes in absorption spectra were firstly observed by UV spectroscopy in the range of 409–420 nm (Fig. 1a). XRD was done for determination of phase composition and crystalline structure of AgNPs. It was found similar to the international database of JCPDS file number no- 04–0783 (Fig. 1e). The size and shape of AgNPs were determined using TEM and Nanoparticle Tracking Analyzer (Fig. 1b) at 100–200 nm scale. The uniform surface structure was observed when AgNPs were further analyzed by SEM at 50 μm scale. The topographic structure of AgNPs surface was found spherical and uniform in (Fig. 1d). It was found that the majority of AgNPs size was found in between 12 and 30 nm in size (Fig. 1d). Further FT-IR analysis was carried out to find out the functional group on AgNPs induced by sodium citrate shows various absorption peaks at 2344.74, 1642.4, 1498, 1385, 1128.45, 899.23, 796.21, 671.02, 627.2, 595.30 and 450.50 cm-1 which represent the functional group such as –NH2, -COOH, CH2, and C═O (Fig. 1c). Several studies have shown similar characteristic UV-Visible peak, SEM and TEM images and diffraction patterns as found in this study [19,20].

The compelling interest of silver nanoparticles in cancer therapeutics is due to its physicochemical characteristics such as large surface area, small size and surface chemistry which differentiate them from bulk Silver. AgNPs constantly release higher magnitude of silver ions (Ag+) than silver microparticles of the same weight [21]. The therapeutic potential of AgNPs is rather dogmatic and is ineffective of their shape and capping material. AgNPs are mostly up taken by endocytosis-related mechanism, after which the organelles are directed to lysosomal fusion. The acidic environment of lysosomes enhances release of silver ions from AgNPs, of which the reactive ions then disturb the cell homeostasis which further leads to apoptotic cell death [22]. Similar to that observed in literature, Citrate based synthesized AgNPs decreased cell proliferation in all cancer cell lines teseted (mentioned below) and thymocytes & splenocytes (Figs. 2 and 3). It can be evidently said that AgNPs showed increased cytotoxicity in splenocytes and thymocytes. A study on the effect of AgNPs on splenocyte activity in mouse have also shown that prolonged administration of Ag-NPs is detrimental on healthy organisms, [23]. The cells were cultured in media with different concentration of AgNPs as given below. The colloidal AgNPs solution was quite stable on addition to the culture media in given concentrations. No agglomeration was observed on addition of AgNPs, as they must have been capped by the proteins present in FBS added to the culture media as reported in literature [24]. It was found that 49.21 μg/ml of AgNPs for DL cells, for PC-3 30.82 μg/ml; MDAMB-231 26.79 μg/ml; MCF-7 9.13 μg/ml; Cal33–6.4 μg/ml (Fig. 2); CSC Cal33–17.6 μg/ml (Fig. 2) dose of AgNPs was effective for inhibition of cell growth. Whereas $IC_{50}$ of thymocytes and splenocytes was found to be significantly lower (0.6426 and 0.1211 μg/ml respectively) as compared to cancer cell lines (Fig. 3). AgNPs showed cytotoxic effect on control cell line HEK 293 T 1.52 μg/ml which is similar to that of reported by [25]. Many studies have also reported that AgNPs made by green synthesis or chemical reduction have a significant role in decreasing Breast [6,26] Prostate [27] cancer and other cancer cell viability in concentration and cell type manner dependent manner. But their effect on cancer stem cell population of cell lines hasn't been documented yet. In this study Cal33

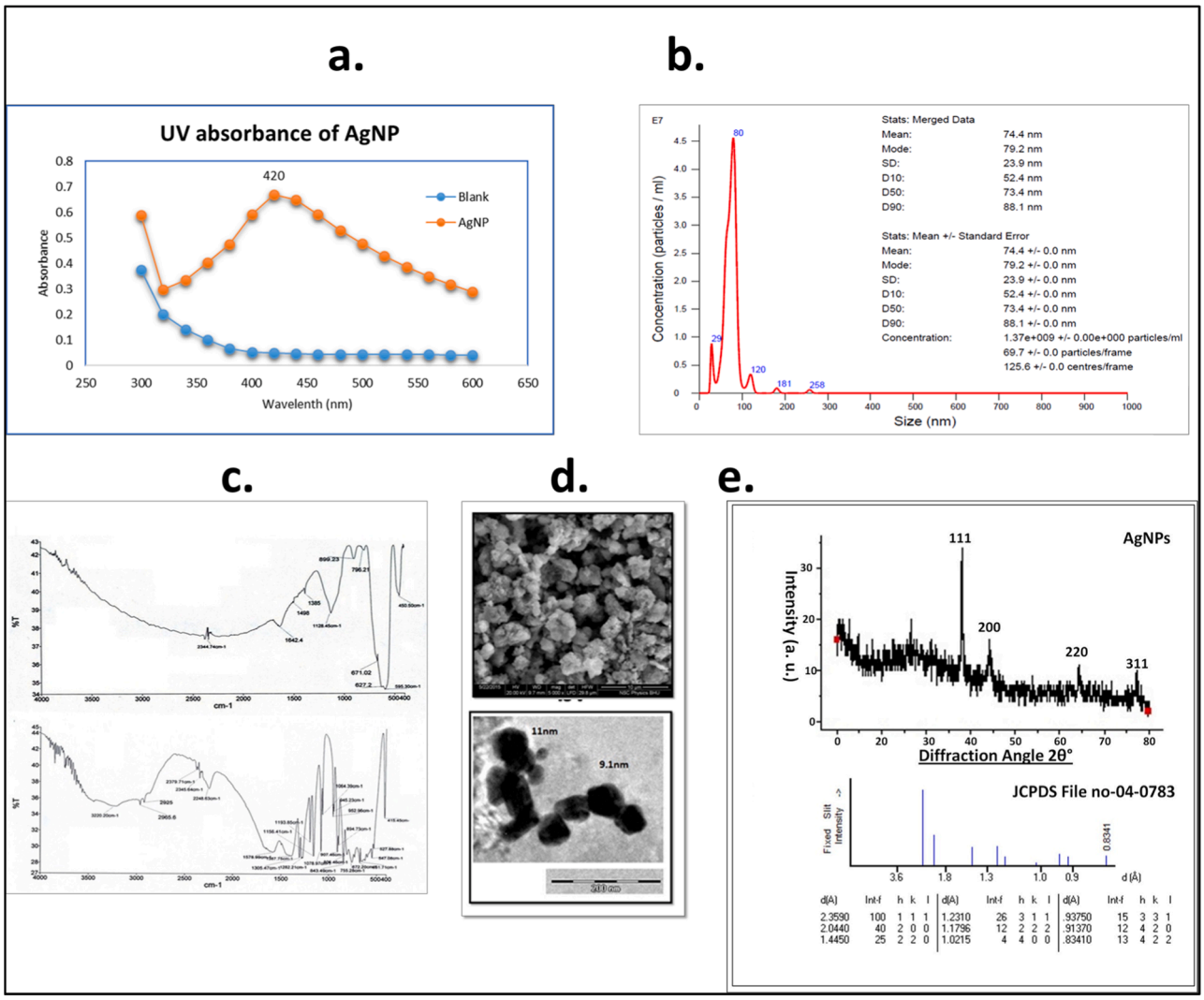


**Fig. 1. a.** UV-Visible spectra of AgNPs showing a characteristic peak at 420 nm wavelength. **b.** NTA graph showing size v/s concentration of AgNPs depicting maximun peak at 80 nm size at 1:100 dilution. **c.** FTIR of AgNPs confirming the presence of carbonyl group on surface of nanoparticles due to capping with citrate ions g. **d.** SEM and TEM images at 1:100 dilution of AgNPs in distilled water confirming the spherical shape of synthesized AgNPs. **e.** Diffraction analysis of AgNPs showing consensus with JCPDS File no 04–0783.

showed least $IC_{50}$ dose among all cancer cell lines, hence it was selected for further experiments.

Cancer Stem cells are known to be more resistant than other cancer cells to verify that, CSCs isolation from Cal33 was carried out. CSCs were isolated from Cal33 with 1.6% recovery. The $CD24^{-/low}$ $CD44^{+}$ CSCs cells were 77.5% after isolation by magnetic sorting as depicted in Fig. 4. In addition to that $CD24^{+}$ cells were reduced to half after sorting, giving a good population of CSCs. MTT assay for determining $IC_{50}$ Value of CSCs was performed. It was shown that CSCs were more resistant to AgNPs treatment with $IC_{50}$ value of 17.55 μg/ml almost 3 times higher than Cal33 cells. Thus, the results so far showed that AgNPs nanoparticles have anti-tumor ability to regress the tumor cell growth while the cancer stem cells are less responsive at lower concentrations.

In order to validate the anti-tumor potential of AgNPs nanoparticles, both Cal33 cells and Cal33 stem cells were treated with AgNPs with their respective $IC_{50}$ doses and Annexin V/PI apoptosis assay and cell cycle assay using flow cytometry were performed. Gating strategy for the same is given in Supplementary Figure 3. It was observed that AgNPs effect viability of both cancer cells and cancer stem cells. AgNP treatment increased percentage of early apoptotic cells by 9.76% and 5.93% and necrotic cells by 6.89% and 4.95% in Cal33 and CSCs respectively (Table 1). It was striking to observe a negligible change in late apoptotic cells (Fig. 6). Studies have shown increase in percentage of early apoptotic cells on Nano-TP (AgNPs synthesized by green extract of Cynara scolymus L. plant) treatment on PC3 cell while A549 cell line showed more increase in late apoptotic cells which is contrary to what is observed in this study [27]. In contrast to our finding a study reported that low doses (5 μg/ml) of Polyvinylpyrrolidone (PVP)-coated AgNPs decreases the apoptotic potential of Tumor necrosis factor-α (a proinflammatory cytokine and apoptosis inducer) in Lung epithelial cell line NCI-H292 [28].

Cell cycle assay also showed resistant behaviors of CSC. Percentage of cells in G1 phase of Cal33 cells was observed to be 45.3% which was significantly higher in case of CSC Cal33 i.e. 53.5% as depicted in Fig. 7 showing a G1/G0 phase arrest. Consequently, less percentage of cells were observed to be in S and G2 phase in case of Cal33 cancer stem cells (25.9% and 19.2%) than Cal33 cells (30.6% and 22.8%) (Table 2). Cell cycle arrest in case of AgNP treatment is reported in various studies showing it to be cell type dependent. The cell cycle arrest in G1/G0 phase has been reported in HSC-4 cells (Human oral squamous carcinoma) [29] while in S phase in BEAS-2B (lung epithelial cell line) and also in G2 phase in A549 (lung carcinoma epithelial cell) [30]. A study on the effect of AgNPs on cell cycle of HeLa cells has reported arrest at S and G2/M phases, while additional subG1 population was observed

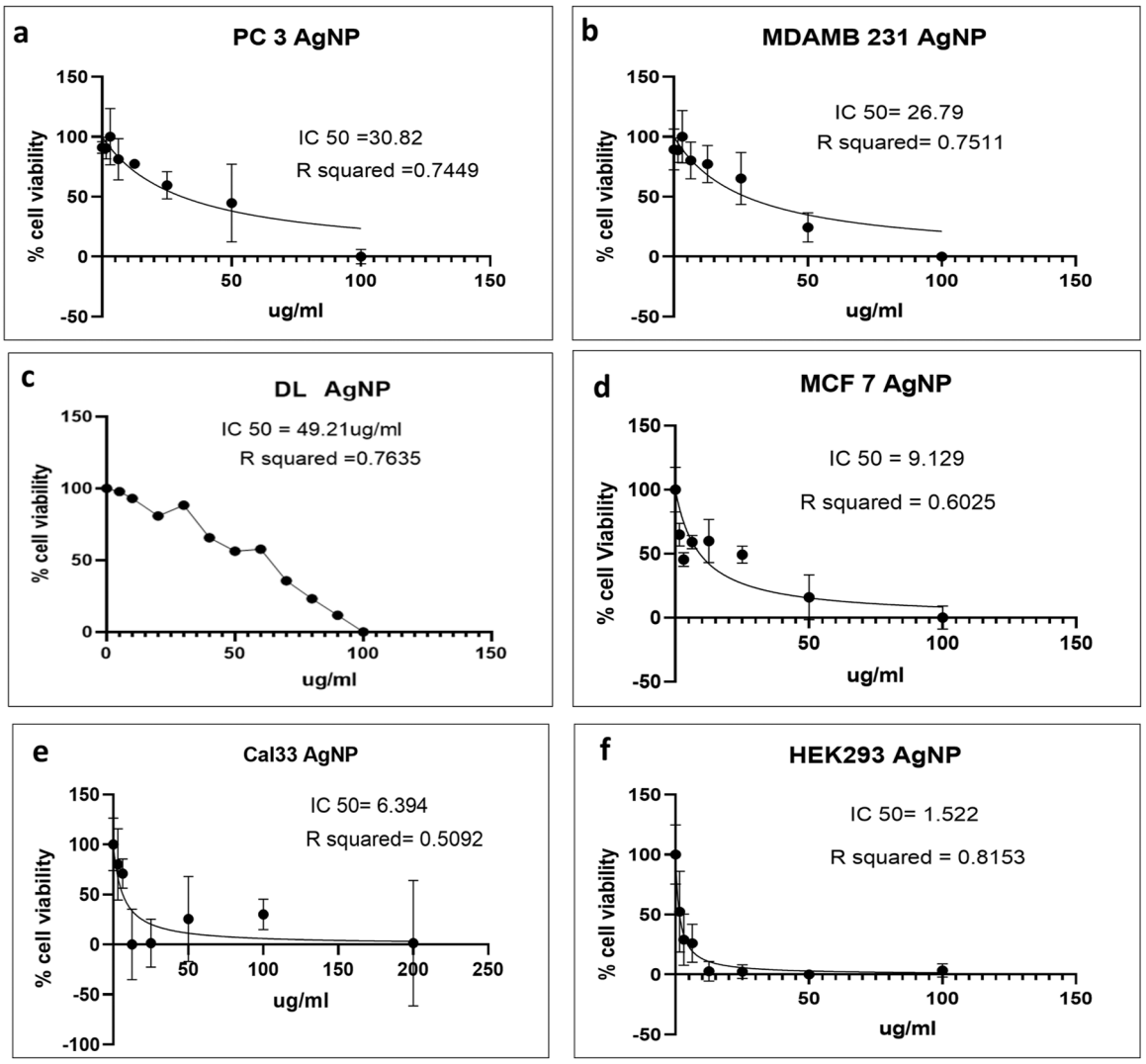


**Fig. 2.** Cell viability % after AgNP treatment of different cell lines **a.** PC 3 with $IC_{50}$ of 30.82 μg/ml, **b.** MDAMB 231 with $IC_{50}$ of 26.79 μg/ml, **c.** DL (Dalton Lymphoma) with $IC_{50}$ of 49.21 μg/ml, **d.** MCF-7 with $IC_{50}$ of 9.129 μg/ml **e.** Cal33, **f.** HEK 293 with $IC_{50}$ of 1.522 μg/ml by MTT assay. After 24 hr incubation with AgNPs.

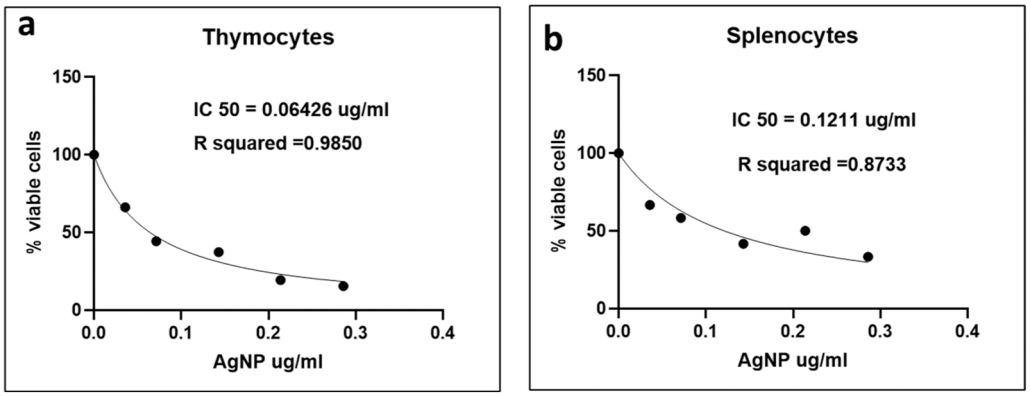


**Fig. 3.** Cell viability % after AgNP treatment of thymocytes and splenocytes by trypan blue assay. Dose dependent decrease in cell viability of Thymocytes $IC_{50}$ = 0.06426 μg/ml and Splenocytes $IC_{50}$ = 0.1211 μg/ml with AgNPs treatment with concentration range 300–30 μg/ml.

which increased with increase in concentration of AgNPs indicating apoptosis or DNA damage [31]. The observed arrest in different phases of cell cycle indicate entry of such cells in cell cycle repair, cells which pass the cell cycle repair checkpoints resume their cycle while others enter an early apoptotic phase which is plausible reason for increased percentage of such cells in case of cancer stem cells on AgNP treatment. So, it can be assumed that nano size of AgNPs treatment must have facilitated to their anti-tumor potential and cell cycle arrest in cancer

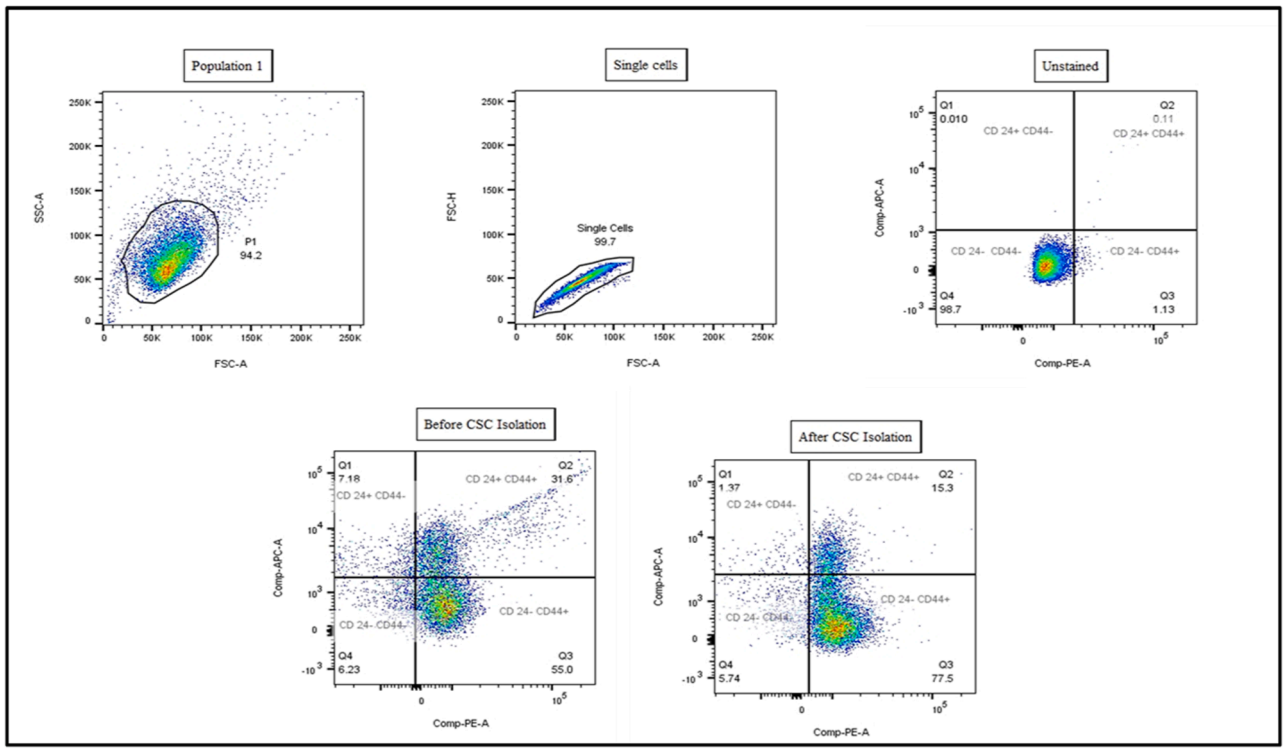


**Fig. 4.** CSC isolated from Cal33 characterization by Flow Cytometry. **Population 1** and **Single cell** dot plots show the gating strategy for events of interest and eliminating doublets and triplets. **Untreated** is a negative control for $CD44^{+}$PE and $CD24^{+}$APC staining. **Before CSC isolation** shows 55% of $CD44^{+}$ and $CD24^{low}$ population. **After CSC isolation** shows $CD44^{+}$ and $CD24^{low}$ to increase up to 77.5%.

**Table 1**
Apoptosis assay comparison in Cancer cells and Cancer stem cells.

| Cell % | Control | Cal33 AgNP Treated | CSC Cal33 AgNP Treated |
|---|---|---|---|
| Live | 96.9% | 77.00% | 82% |
| Necrotic | 1.55% | 8.44% | 6.5% |
| Early apoptotic | 1.24% | 11.00% | 7.17% |
| Late apoptotic | 0.26% | 3.57% | 3.5% |

*Cancer stem cells (CSC Cal33)

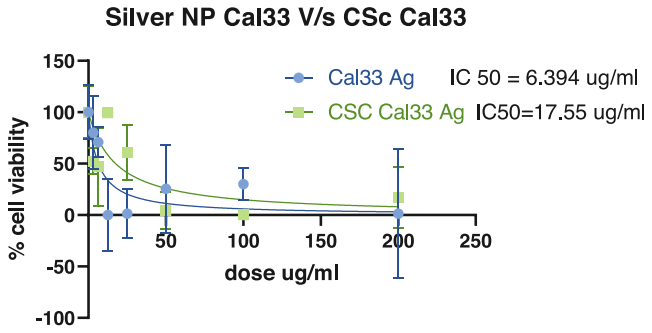


**Fig. 5.** $IC_{50}$ comparison of Cal33 and CSC Cal33 on AgNP treatment. Dose dependent inhibitory effect of AgNPs (3.125 μg/ml- 200 μg/ml) on both Cal33 (shown in blue) $IC_{50}$ = 6.394 μg/ml and CSCs Cal33 (shown in blue) $IC_{50}$ = 17.55 μg/ml. MTT assay was performed after 24 hr incubation with AgNPs.

and cancer stem cells.

## 4. Conclusion

All techniques used for the characterization showed successful formation of AgNPs. AgNPs displayed anti-tumor role in all cancer cell lines i.e., Cal33, PC-3, DL and MDAMB231. Some off target cytotoxic effects on normal cells such as HEK 293, splenocytes and thymocytes was also observed. Cal33 was most sensitive to AgNPs among all cancer cell lines responding to lowest inhibitory concentration of silver nanoparticles. Increased resistance to AgNPs was observed in Cal33 Cancer stem cells as inhibitory concentrations was thrice than that of Cal 33. The mechanism behind apoptosis was observed to be cell cycle arrest in CSC Cal33 and Cal33 cells. Some further experiments are required to better understand the mode of action of AgNPs such that its off-target effects are minimized and a low dosage can be optimized for targeting cancer and cancer stem cells. Although, AgNPs have shown potential as an anticancer agent but its cytotoxicity to normal cells cannot be neglected. In, addition to that, its resistance in cancer stem cells needs to considered while furthering nanotherapeutics.

## CRediT authorship contribution statement

**Rupinder Kaur** performed the major wet lab experiments, analyzed and interpreted the data and wrote the manuscript. **Khushwant Singh** and **Sonam Agarwal**: assisted in some of the wet lab experiments relating flowcytometry and mouse handling, contributed reagents, materials, analysis tools or data and analyzed and interpreted the data. **Marilyn Masih** and **Anita Chauhan**: performed the proofreading of the manuscript along with verifying and arranging the references. **Pramod Kumar Gautam**: Conceived and designed the experiments and provided expert technical guidance and evaluated the manuscript.

## Declaration of Competing Interest

The authors declare that they have no known competing financial interests or personal relationships that could have appeared to influence the work reported in this paper. No conflict of interest.

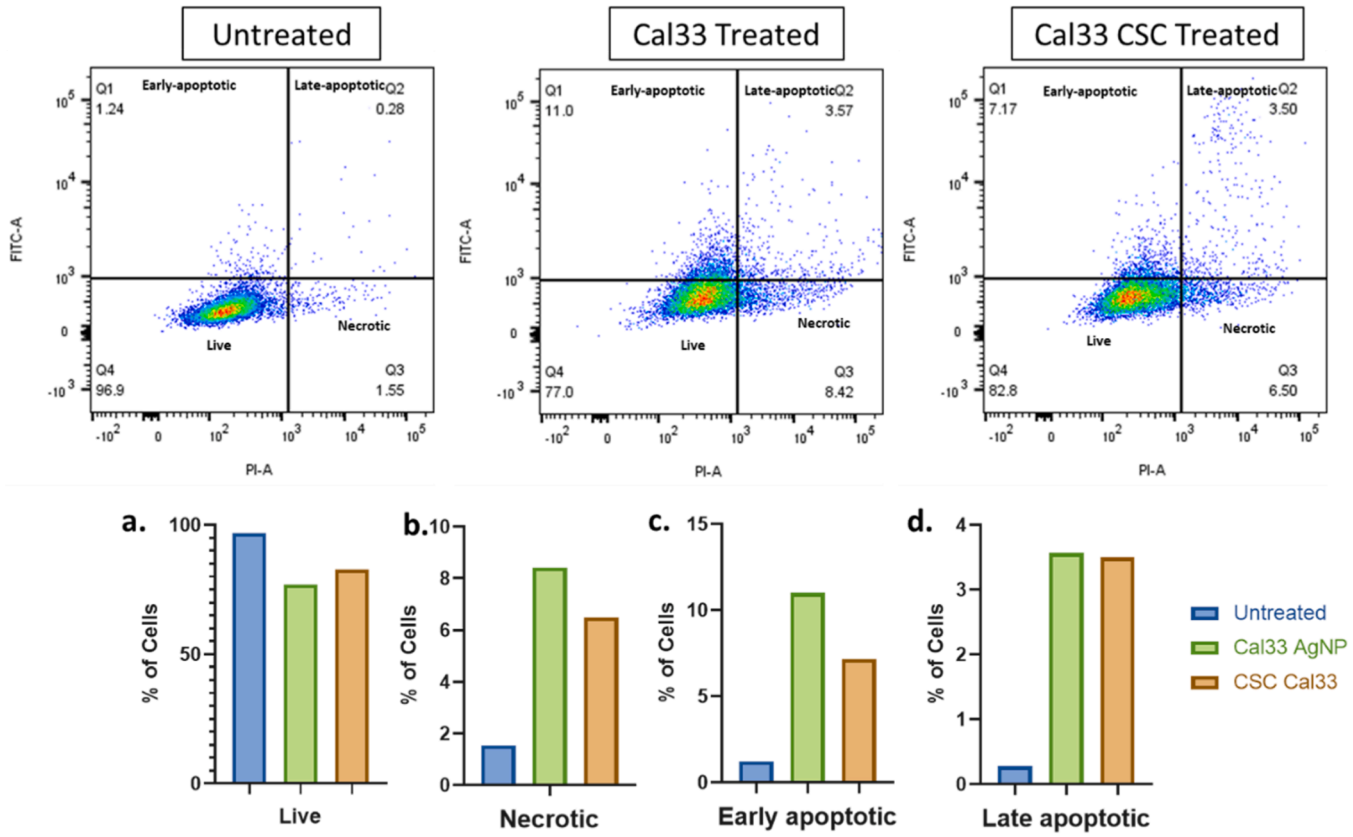


**Fig. 6.** Apoptosis assay comparison of Cal33 and CSC Cal33 on AgNP treatment. **a.** Percentage of live cells **b.** Percentage of Necrotic cells **c.** Percentage of Early apoptotic cells. **d.** Percentage of Late of apoptotic cells in three groups Untreated, Cal33and CSC Cal33 AgNP treated cells.

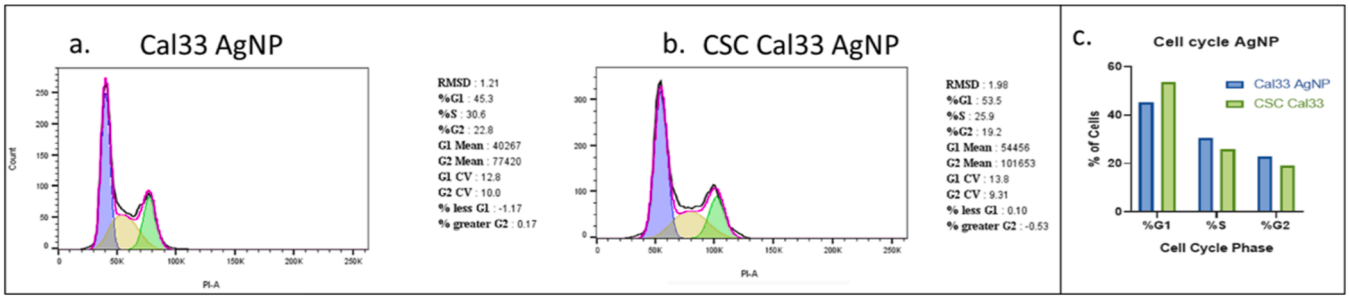


**Fig. 7.** Cell Cycle comparison of Cal33 and CSC Cal33 on AgNP treatment. **a. Cal33** cell cycle plot with %G1 45.3, %S 30.6, %G2 22.8. **b. CSC Cal33** cell cycle plot with %G1 53.5, %S 25.9, %G2 19.2. **c.** Bar graph showing comparison of different cell cycle phases of Cal33 and CSC Cal33. Cell cycle analysis was done using Dean-Jett-Fox model of FlowJo software.

**Table 2**
Cell cycle phase comparison in Cancer cells and Cancer stem cells.

| Cell Cycle | Cal33 | CSC Cal33 |
|---|---|---|
| G1/G0 | 45.30% | 53.50% |
| S | 30.60% | 25.90% |
| G2/M | 22.80% | 19.20% |

*Cancer stem cells (CSC Cal33)

## Data availability

Data will be made available on request.

## Acknowledgments

The authors acknowledge the financial support by DST SERB, India (Project –EEQ/2018/000785), and infrastructure facilities by All India Institute of Medical Sciences, New Delhi, India. We also acknowledge the facility of Nanosight instrument provided by Dr. AK Dhinda, Professor Department of Pathology, Convergence Block, AIIMS, New Delhi.

## Appendix A. Supporting information

Supplementary data associated with this article can be found in the online version at doi:10.1016/j.toxrep.2023.11.008.

## References

[1] Cancer, (n.d.). ⟨https://www.who.int/health-topics/cancer#tab=tab_1⟩ (accessed November 12, 2023).
[2] Y. He, B. Xu, W. Li, H. Yu, Silver nanoparticle-based chemiluminescent sensor array for pesticide discrimination, J. Agric. Food Chem. 63 (2015) 2930–2934, https://doi.org/10.1021/ACS.JAFC.5B00671.

[3] A. Saxena, R.M. Tripathi, F. Zafar, P. Singh, Green synthesis of silver nanoparticles using aqueous solution of Ficus benghalensis leaf extract and characterization of their antibacterial activity, Mater. Lett. 67 (2012) 91–94, https://doi.org/10.1016/J.MATLET.2011.09.038.
[4] D. Kovács, N. Igaz, M.K. Gopisetty, M. Kiricsi, Cancer therapy by silver nanoparticles: fiction or reality? Int. J. Mol. Sci. 23 (2022) https://doi.org/10.3390/IJMS23020839.
[5] K. Ranoszek-Soliwoda, E. Tomaszewska, E. Socha, P. Krzyczmonik, A. Ignaczak, P. Orlowski, M. Krzyzowska, G. Celichowski, J. Grobelny, The role of tannic acid and sodium citrate in the synthesis of silver nanoparticles, J. Nanopart. Res. 19 (2017), https://doi.org/10.1007/S11051-017-3973-9.
[6] P.R. Hemlata, A.P. Meena, K.K.Tejavath Singh, Biosynthesis of silver nanoparticles using cucumis prophetarum aqueous leaf extract and their antibacterial and antiproliferative activity against cancer cell lines, ACS Omega 5 (2020) 5520–5528, https://doi.org/10.1021/ACSOMEGA.0C00155.
[7] A. Sangtani, E. Petryayeva, K. Susumu, E. Oh, A.L. Huston, G. Lasarte-Aragones, I. L. Medintz, W.R. Algar, J.B. Delehanty, Nanoparticle-peptide-drug bioconjugates for unassisted defeat of multidrug resistance in a model cancer cell line, Bioconjug Chem. 30 (2019) 525–530, https://doi.org/10.1021/ACS.BIOCONJCHEM.8B00755.
[8] Y. Yao, Y. Zhou, L. Liu, Y. Xu, Q. Chen, Y. Wang, S. Wu, Y. Deng, J. Zhang, A. Shao, Nanoparticle-based drug delivery in cancer therapy and its role in overcoming drug resistance, Front Mol. Biosci. 7 (2020), https://doi.org/10.3389/FMOLB.2020.00193.
[9] W. Liu, X. Li, Y.S. Wong, W. Zheng, Y. Zhang, W. Cao, T. Chen, Selenium nanoparticles as a carrier of 5-fluorouracil to achieve anticancer synergism, ACS Nano 6 (2012) 6578–6591, https://doi.org/10.1021/NN202452C/SUPPL_FILE/NN202452C_SI_001.PDF.
[10] A. Kuşoğlu, Ç. Biray Avcı, Cancer stem cells: a brief review of the current status, Gene 681 (2019) 80–85, https://doi.org/10.1016/J.GENE.2018.09.052.
[11] L. Walcher, A.K. Kistenmacher, H. Suo, R. Kitte, S. Dluczek, A. Strauß, A. R. Blaudszun, T. Yevsa, S. Fricke, U. Kossatz-Boehlert, Cancer stem cells-origins and biomarkers: perspectives for targeted personalized therapies, Front Immunol. 11 (2020), https://doi.org/10.3389/FIMMU.2020.01280.
[12] Y.J. Choi, J.H. Park, J.W. Han, E. Kim, O. Jae-Wook, S.Y. Lee, J.H. Kim, S. Gurunathan, Differential cytotoxic potential of silver nanoparticles in human ovarian cancer cells and ovarian cancer stem cells, Int. J. Mol. Sci. 17 (2016), https://doi.org/10.3390/IJMS17122077.
[13] J.W. Han, S. Gurunathan, Y.J. Choi, J.H. Kim, Dual functions of silver nanoparticles in F9 teratocarcinoma stem cells, a suitable model for evaluating cytotoxicity- and differentiation-mediated cancer therapy, Int. J. Nanomed. 12 (2017) 7529–7549, https://doi.org/10.2147/IJN.S145147.
[14] S. Agarwal, A. Chauhan, K. Singh, K. Kumar, R. Kaur, M. Masih, P.K. Gautam, Immunomodulatory effects of β-defensin 2 on macrophages induced immuno-upregulation and their antitumor function in breast cancer, BMC Immunol. 23 (2022), https://doi.org/10.1186/S12865-022-00527-Y.
[15] M. Zarei, E. Karimi, E. Oskoueian, A. Es-Haghi, M.E.T. Yazdi, Comparative study on the biological effects of sodium citrate-based and apigenin-based synthesized silver nanoparticles, Nutr. Cancer 73 (2021) 1511–1519, https://doi.org/10.1080/01635581.2020.1801780.
[16] S.H. Lee, B.H. Jun, Silver nanoparticles: synthesis and application for nanomedicine, 2019, Vol. 20, Page 865, Int. J. Mol. Sci. 20 (2019) 865, https://doi.org/10.3390/IJMS20040865.
[17] P.K. Gautam, S. Kumar, M.S. Tomar, R.K. Singh, A. Acharya, S. Kumar, B. Ram, Selenium nanoparticles induce suppressed function of tumor associated macrophages and inhibit Dalton's lymphoma proliferation, Biochem Biophys. Rep. 12 (2017) 172–184, https://doi.org/10.1016/J.BBREP.2017.09.005.
[18] Y.G. Yuan, S. Zhang, J.Y. Hwang, I.K. Kong, Silver nanoparticles potentiates cytotoxicity and apoptotic potential of camptothecin in human cervical cancer cells, Oxid. Med Cell Longev. 2018 (2018), https://doi.org/10.1155/2018/6121328.
[19] Y.G. Yuan, Q.L. Peng, S. Ggurunathan, Silver nanoparticles enhance the apoptotic potential of gemcitabine in human ovarian cancer cells: combination therapy for effective cancer treatment, Int J. Nanomed. 12 (2017) 6487–6502, https://doi.org/10.2147/IJN.S135482.
[20] D. Chicea, A. Nicolae-Maranciuc, A.S. Doroshkevich, L.M. Chicea, O.M. Ozkendir, Comparative synthesis of silver nanoparticles: evaluation of chemical reduction procedures, AFM and DLS size analysis, 2023, Vol. 16, Page 5244, Materials 16 (2023) 5244, https://doi.org/10.3390/MA16155244.
[21] G. Schneider, Antimicrobial silver nanoparticles – regulatory situation in the European Union, Mater. Today Proc. 4 (2017) S200–S207, https://doi.org/10.1016/J.MATPR.2017.09.187.
[22] S.J. Cameron, F. Hosseinian, W.G. Willmore, A current overview of the biological and cellular effects of nanosilver, 2018, Vol. 19, Page 2030, Int. J. Mol. Sci. 19 (2018) 2030, https://doi.org/10.3390/IJMS19072030.
[23] J. Małaczewska, The effect of silver nanoparticles on splenocyte activity and selected cytokine levels in the mouse serum at early stage of experimental endotoxemia, Pol. J. Vet. Sci. 14 (2011), https://doi.org/10.2478/V10181-011-0089-5.
[24] D. Mahl, C. Greulich, W. Meyer-Zaika, M. Köller, M. Epple, Gold nanoparticles: dispersibility in biological media and cell-biological effect, J. Mater. Chem. 20 (2010) 6176–6181, https://doi.org/10.1039/C0JM01071E.
[25] M. Bin-Jumah, M. Al-Abdan, G. Albasher, S. Alarifi, Effects of green silver nanoparticles on apoptosis and oxidative stress in normal and cancerous human hepatic cells in vitro, Int. J. Nanomed. 15 (2020) 1537–1548, https://doi.org/10.2147/IJN.S239861.
[26] B. Plackal Adimuriyil George, N. Kumar, H. Abrahamse, S.S. Ray, Apoptotic efficacy of multifaceted biosynthesized silver nanoparticles on human adenocarcinoma cells, Sci. Rep. 8 (2018), https://doi.org/10.1038/S41598-018-32480-5.
[27] A.I.M. Khedr, M.S. Goda, A.F.S. Farrag, A.M. Nasr, S.A. Swidan, M.S. Nafie, M. S. Abdel-Kader, J.M. Badr, R.F.A. Abdelhameed, Silver nanoparticles formulation of flower head's polyphenols of cynara scolymus L.: a promising candidate against prostate (PC-3) cancer cell line through apoptosis activation, Molecules 27 (2022), https://doi.org/10.3390/MOLECULES27196304.
[28] A. Fehaid, A. Taniguchi, Silver nanoparticles reduce the apoptosis induced by tumor necrosis factor-α, Sci. Technol. Adv. Mater. 19 (2018) 526, https://doi.org/10.1080/14686996.2018.1487761.
[29] F. Yakop, S.A. Abd Ghafar, Y.K. Yong, L. Saiful Yazan, R. Mohamad Hanafiah, V. Lim, Z. Eshak, Silver nanoparticles Clinacanthus Nutans leaves extract induced apoptosis towards oral squamous cell carcinoma cell lines, Artif. Cells Nanomed. Biotechnol. 46 (2018) 131–139, https://doi.org/10.1080/21691401.2018.1452750.
[30] R.J. Holmila, S.A. Vance, S.B. King, A.W. Tsang, R. Singh, C.M. Furdui, Silver nanoparticles induce mitochondrial protein oxidation in lung cells impacting cell cycle and proliferation, Antioxidants 8 (2019), https://doi.org/10.3390/ANTIOX8110552.
[31] E. Panzarini, S. Mariano, C. Vergallo, E. Carata, G.M. Fimia, F. Mura, M. Rossi, V. Vergaro, G. Ciccarella, M. Corazzari, L. Dini, Glucose capped silver nanoparticles induce cell cycle arrest in HeLa cells, Toxicol. Vitr. 41 (2017) 64–74, https://doi.org/10.1016/J.TIV.2017.02.014.